

Centennial Channel Response to Climate Change in an Engineered River

Ylla Arbós, C.; Blom, A.; Sloff, C. J.; Schielen, R. M. J.

DOI

[10.1029/2023GL103000](https://doi.org/10.1029/2023GL103000)

Publication date

2023

Document Version

Final published version

Published in

Geophysical Research Letters

Citation (APA)

Ylla Arbós, C., Blom, A., Sloff, C. J., & Schielen, R. M. J. (2023). Centennial Channel Response to Climate Change in an Engineered River. *Geophysical Research Letters*, *50*(8), Article e2023GL103000. <https://doi.org/10.1029/2023GL103000>

Important note

To cite this publication, please use the final published version (if applicable). Please check the document version above.

Copyright

Other than for strictly personal use, it is not permitted to download, forward or distribute the text or part of it, without the consent of the author(s) and/or copyright holder(s), unless the work is under an open content license such as Creative Commons.

Takedown policy

Please contact us and provide details if you believe this document breaches copyrights. We will remove access to the work immediately and investigate your claim.




Geophysical Research Letters®



RESEARCH LETTER

10.1029/2023GL103000

Centennial Channel Response to Climate Change in an Engineered River

C. Ylla Arbós¹ , A. Blom¹ , C. J. Sloff^{1,2}, and R. M. J. Schielen^{1,3} 

¹Faculty of Civil Engineering and Geosciences, Delft University of Technology, Delft, The Netherlands, ²Deltares, Delft, The Netherlands, ³Ministry of Infrastructure and Water Management, DG Rijkswaterstaat, Utrecht, The Netherlands

Key Points:

- Human intervention will continue to govern channel response in the lower Rhine River by 2100, mainly through channel bed incision
- Climate change leads to sea level rise and hydrograph adjustment, the latter being dominant and causing enhanced incision
- Channel response to human intervention slows down as the river approaches its equilibrium state, but response to climate change accelerates

Supporting Information:

Supporting Information may be found in the online version of this article.

Correspondence to:

C. Ylla Arbós,
c.yllaarbos@tudelft.nl

Citation:

Ylla Arbós, C., Blom, A., Sloff, C. J., & Schielen, R. M. J. (2023). Centennial channel response to climate change in an engineered river. *Geophysical Research Letters*, 50, e2023GL103000. <https://doi.org/10.1029/2023GL103000>

Received 24 JAN 2023

Accepted 12 APR 2023

Author Contributions:

Conceptualization: C. Ylla Arbós, A. Blom, R. M. J. Schielen
Data curation: C. Ylla Arbós
Formal analysis: C. Ylla Arbós, A. Blom
Funding acquisition: A. Blom, R. M. J. Schielen
Methodology: C. Ylla Arbós, A. Blom, R. M. J. Schielen
Project Administration: R. M. J. Schielen
Resources: A. Blom, C. J. Sloff, R. M. J. Schielen
Software: C. Ylla Arbós, C. J. Sloff
Supervision: A. Blom, R. M. J. Schielen

© 2023. The Authors.

This is an open access article under the terms of the [Creative Commons Attribution-NonCommercial-NoDerivs License](https://creativecommons.org/licenses/by/4.0/), which permits use and distribution in any medium, provided the original work is properly cited, the use is non-commercial and no modifications or adaptations are made.

Abstract Human intervention makes river channels adjust their slope and bed surface grain size as they transition to a new equilibrium state in response to engineering measures. Climate change alters the river controls through hydrograph changes and sea level rise. We assess how channel response to climate change compares to channel response to human intervention over this century (2000–2100), focusing on a 300-km reach of the Rhine River. We set up a schematized numerical model representative of the current (1990–2020), non-graded state of the river, and subject it to scenarios for the hydrograph, sediment flux, and sea level rise. We conclude that the lower Rhine River will continue to adjust to past channelization measures in 2100 through channel bed incision. This response slows down as the river approaches its new equilibrium state. Channel response to climate change is dominated by hydrograph changes, which increasingly enhance incision, rather than sea level rise.

Plain Language Summary Humans have modified rivers to enable boat traffic, to protect people against flooding, and to provide them with freshwater and energy. When the shape of a river changes, the amount of sand and gravel (sediment) that can move along its bed also changes. In response, rivers change their slope and bed characteristics, so that they can transport as much sediment as they receive from higher up in the basin. This results in changes in bed level, which becomes higher or lower, causing problems for navigation and flood protection. Climate change makes this worse, because it changes the amount of water flowing down the river, and sea level. This further affects the amount of sediment that can move down the river, therefore causing additional bed level change. Here we study how climate change affects the lower Rhine River (Germany-Netherlands), over the 21st century. This river has been heavily modified by humans, and its bed has been lowering over hundreds of kilometers. With a computer model, we simulate how different scenarios of climate change affect this behavior. We foresee that the ongoing bed level lowering will continue in the upcoming decades, and that it will be enhanced by climate change.

1. Introduction

River engineering measures such as channelization, diversion, and dam construction, alter the equilibrium state of rivers, triggering an adjustment toward the new equilibrium state (Blom et al., 2016; De Vriend, 2015; Mackin, 1948). In engineered rivers with a fixed planform, this response is limited to (a) channel slope adjustment through channel incision or aggradation, and (b) changes in the bed surface grain size distribution. The magnitude, extent, and timescale of channel response to engineering measures can add up to meters of bed level change, extend over hundreds of kilometers, and take decades to centuries (De Vriend, 2015).

Climate change alters the river controls through changes in precipitation, ice- and snow-melt, and sea level rise, which modifies the hydrograph (Blöschl et al., 2019; Milliman et al., 2008), sediment supply (Liu et al., 2013; Verhaar et al., 2011), and base level (Chen et al., 2017; IPCC, 2022). Changes in the river controls modify the equilibrium state of the river, prompting channel adjustment. With increasing rates of climate change, the relative influence of climatic controls on channel response becomes ever more important.

Field and modeling studies on channel response to interventions are abundant (e.g., Arkesteijn et al., 2021; Czapiga et al., 2022; Gao et al., 2020; Surian & Rinaldi, 2003; Verhaar et al., 2011; Zaprowski et al., 2005). Large-scale studies of channel response to overall climate change are scarce, and do not typically address the relative magnitude of climate-related and intervention-related changes. Yet climate change affects all of the river controls simultaneously, and many engineered rivers still feature an ongoing response to past human intervention over hundreds of kilometers (Emerson, 1971; Harmar et al., 2005; Surian & Rinaldi, 2003; Ylla Arbós et al., 2021).

Validation: A. Blom, R. M. J. Schielen
Visualization: C. Ylla Arbós
Writing – original draft: C. Ylla Arbós
Writing – review & editing: A. Blom, C. J. Sloff, R. M. J. Schielen

We focus on the lower Rhine River, a 300-km transboundary reach of the Rhine River between Bonn (Germany) and Vuren (The Netherlands), including a bifurcation near the German-Dutch border (Figure 1). The lower Rhine River is a paradigmatic engineered river with a long history of human intervention (Ylla Arbós et al., 2021). The mean water discharge and annual peak flow at Köln are, respectively, 2,155 and 6,450 m³/s. Decades of field data on bed level and bed surface grain size show that the river channel is still adjusting to domain-wide narrowing and shortening measures carried out over the past century (about 30% width reduction and 10% length reduction), as well as to more recent measures (Czapiga et al., 2022; Quick et al., 2019; Ylla Arbós et al., 2021).

Our objective is to assess how climate forcing adds to the ongoing channel response, in terms of bed level and bed surface grain size change, over the period 2000–2100. To this end, we set up a highly schematized numerical model, and subject it to multiple scenarios for climate-related hydrograph changes, sediment flux, and sea level rise.

2. A Schematized Model of Centennial Channel Response

Given the spatio-temporal scale of our study, as well as the uncertainty associated with climate predictions and field data, we aim to identify the type and order of magnitude of channel response to scenarios of climate-related control change. We do not address short-term natural variability of the system, nor local width variations and local effects of structures. We use a one-dimensional model, as we focus on large-scale, order-of-magnitude changes over a century.

The schematization of a complex system to a one-dimensional problem is a balancing act between simplification and representativeness (Paola, 2011): the model needs to capture the main components of channel response, which is best done with a highly schematized model, and at the same time be representative of the lower Rhine River.

We set up a one-dimensional (i.e., cross-section-averaged) morphodynamic model, suitable for mixed-size sediment. The numerical solver is SOBEK-RE (Deltares, 2012a, 2012b). Flow is computed using the steady solution of the shallow water equations (De Saint-Venant, 1871); bed level change is solved through mass conservation of bed sediment (Exner, 1925, 1931), and changes in bed surface grain size are computed through conservation of each grain size class for a surface layer (Hirano, 1971). Sediment transport is calculated with a relation which includes a threshold of motion and accounts for hiding and exposure effects. Further details on the sediment transport relation and model assumptions are provided in Text S1 in Supporting Information S1.

Non-erodible reaches (fixed layers) are modeled as sediment that is sufficiently coarse to be immobile under the prevailing flow conditions. In the field, “summer levees” (relatively low-elevation levees between main channel and floodplain) reduce the occurrence of floodplain flow for, for instance, agricultural reasons. The model does not account for these summer levees, for simplicity reasons and because their effects are mostly relevant in cases with abrupt width changes (e.g., Van Vuren et al., 2015), which do not occur in our model.

Given our focus on bed material load, and following data availability, we consider five grain size classes: fine sand, coarse sand, fine gravel, and two coarse gravel fractions, with characteristic diameters in the order of 0.5, 1.25, 5, 15, and 40 mm, respectively. The bed surface is coarser than the substrate (Frings et al., 2014).

The model initial state is based on the period 1990–2020, and follows smoothed bathymetric and bed surface grain size data (Figures 2a–2c). The initial state covers a relatively long period due to the large natural variability of the data and data availability. This is not problematic as most system properties do not change significantly over this time frame on the large scale. Full details on the model schematization are provided in Text S2 in Supporting Information S1.

As we focus on channel response to changes in the boundary conditions, model boundaries constitute an essential part of our domain of interest. We define three external boundary conditions (water discharge and grain size-specific sediment fluxes upstream, and base level downstream), and an internal nodal condition (sediment partitioning at the bifurcation).

We adopt a cycled hydrograph of daily discharge with a 20-year period, which allows us to account for the natural variability of water discharge while adding a climate signal to it. The hydrograph must capture the flow duration curve, as it governs the mean channel response, while the sequence of flow events determines the fluctuations

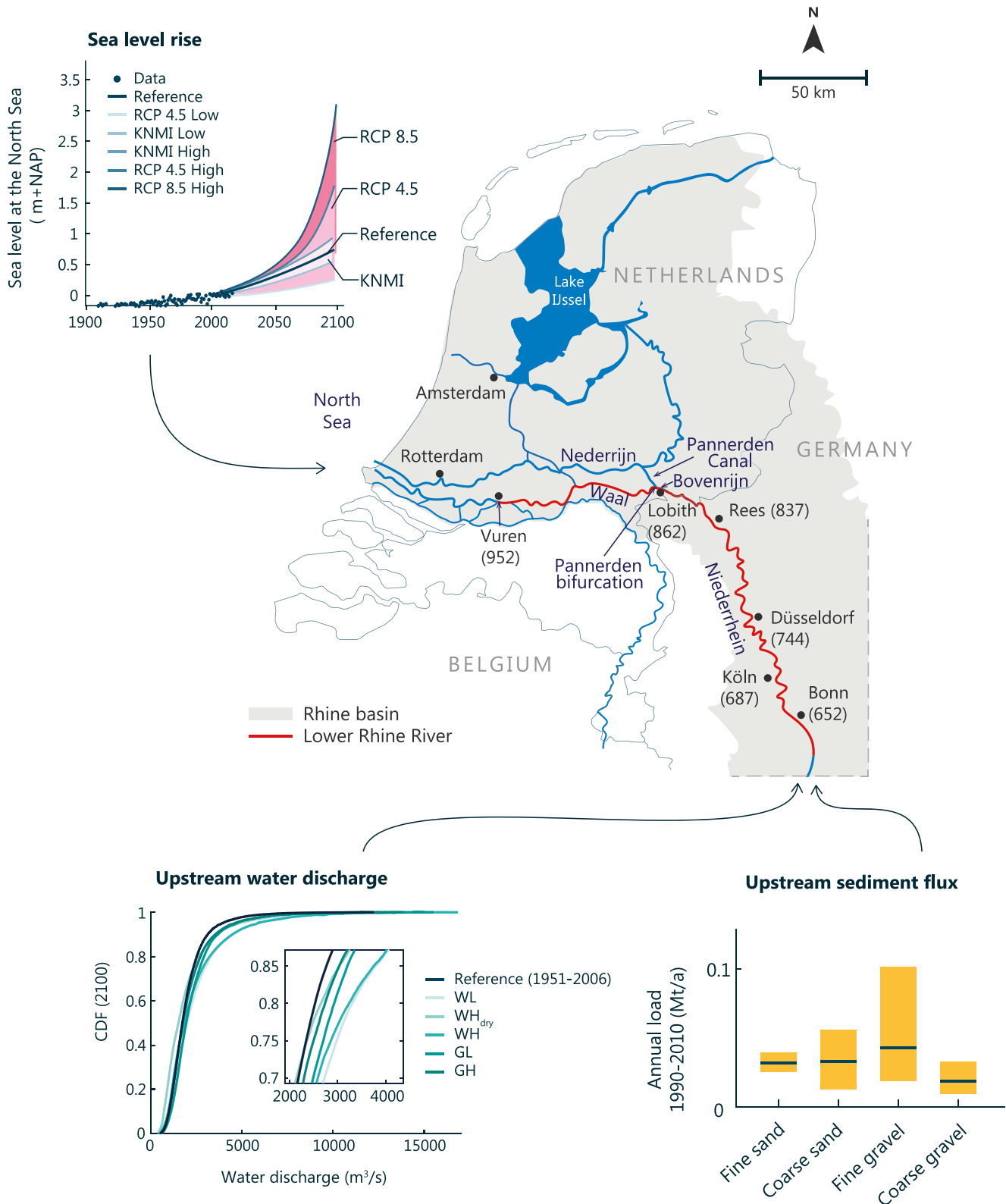


Figure 1. The lower Rhine River between Bonn (Germany) and Vuren (The Netherlands), with scenarios for change of the river controls over the 21st century. Numbers between parentheses indicate river km. Water discharge scenarios follow Sperna Weiland et al. (2015); sea level rise scenarios follow IPCC (2013) and KNMI (2015); sediment flux follows the Frings et al. (2014) uncertainty estimates (mean values in blue, yellow boxes for the 95% confidence interval).

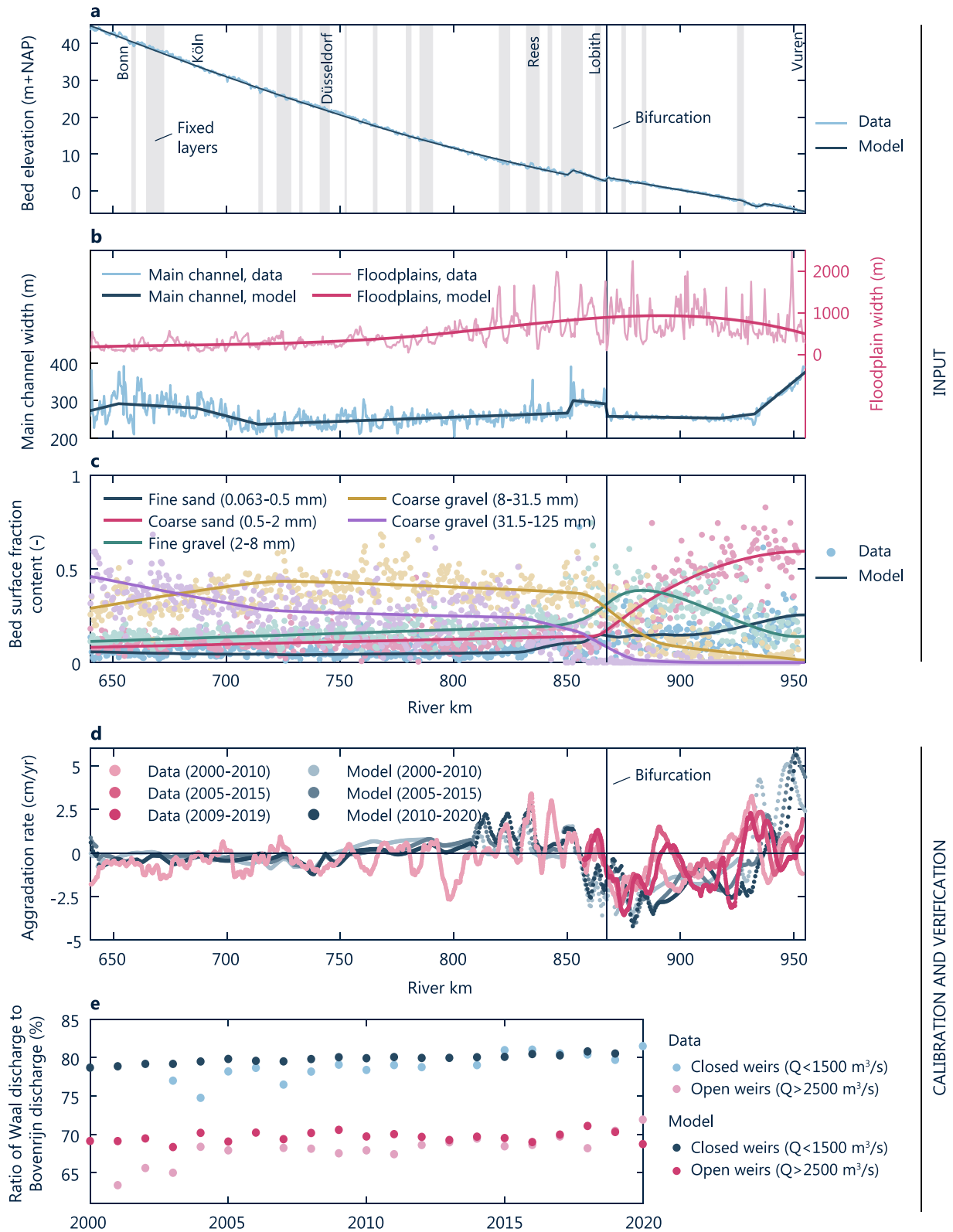


Figure 2. Initial state of the model based on the period 1990–2020 (a–c) and model calibration and verification (d–e): (a) mean main channel bed elevation; (b) main channel and floodplain width; (c) bed surface fraction content of each grain size class; (d) channel bed aggradation rates (5-km moving average); and (e) temporal variation of flow partitioning at the Pannerden bifurcation, represented by the ratio of Waal discharge to Bovenrijn discharge.

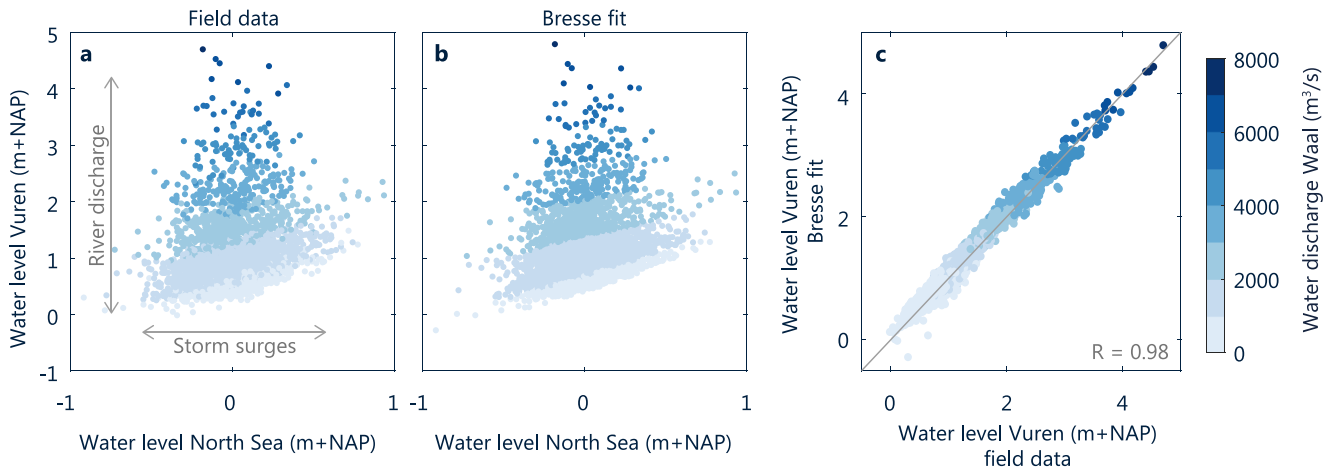


Figure 3. Water level at the downstream boundary of our model (Vuren, river km 952) as a function of water level at the North Sea: (a) field data averaged over 2 days, for the period 1990–2020; (b) De Vries (1994) empirical fit to the Bresse (1860) solution to the backwater equation; and (c) goodness of fit, with R the correlation coefficient.

around it (Arkesteijn et al., 2019, 2021). We select a 20-year period from the historical record (1967–1986) such that its statistics (10th, 50th, and 90th percentiles, mean and standard deviation) best match those of the long-term time series (1951–2006, which is equal to the reference period used in the Sperna Weiland et al. (2015) climate scenario studies).

The upstream sediment flux is set as a function of discharge using the sediment transport relation, scaled such that the annual mean sediment flux per grain size fraction at the upstream boundary resembles the normal-flow load distribution (Blom et al., 2017), and falls within the 95% confidence interval of the Frings et al. (2014) sediment flux estimates (Figure 1). With a discharge-dependent sediment load resembling the normal-flow load distribution, we avoid the presence of an upstream boundary segment over the upstream part of our domain (Blom et al., 2017). We split the flux of the Frings et al. (2014) coarsest fraction in two, proportionally to their substrate content (Parker et al., 1982; Parker & Klingeman, 1982) following field data (Text S2 in Supporting Information S1), as the hiding-exposure relation requires a limited difference between characteristic diameters of the grain size classes.

The downstream boundary (Vuren, river km 952) is located upstream of the estuarine zone, at about 100 km upstream of the North Sea (Figure 1), as our model does not include estuary dynamics such as tides and salt intrusion. Water level at Vuren depends on river discharge and sea level (Figure 3a). We approximate water level at Vuren using the De Vries (1994) empirical fit to the Bresse (1860) analytical solution to the backwater equation. As the normal flow depth d_e is a function of $Q^{2/3}$ (with Q the water discharge), the De Vries (1994) empirical fit equals (see Text S3 in Supporting Information S1 for its derivation)

$$d_v = \Lambda Q^{2/3} + (d_s - \Lambda Q^{2/3}) 2^{KQ^{2/9}/d_s^{4/3}} \quad (1)$$

where d_v denotes flow depth at Vuren, d_s denotes flow depth at the North Sea, and Λ and K are assumed to be constants. We find the highest correlation between field data and Equation 1 for $\Lambda = 0.054 \text{ s}^{2/3}/\text{m}$ and $K = -0.71 \text{ m}^{2/3}\text{s}^{2/9}$ (Figures 3b and 3c).

We include sea level rise at a rate corresponding to the centerline of the KNMI (2015) projections (Figure 1). We assume that water level increase at Vuren due to coastal storm surges and tidal constituents (Figure 3a) is a proxy for water level increase due to sea level rise.

As we use a one-dimensional numerical model, an internal nodal condition sets the sediment partitioning over the two bifurcates. Sediment partitioning at a bifurcation located on a river bend is governed by three-dimensional processes (e.g., Frings & Kleinans, 2008; Sloff & Mosselman, 2012), which cannot be represented in a one-dimensional model. For each grain size class, the sediment partitioning is prescribed by a nodal point relation (Bolla Pittaluga et al., 2003; Schielen & Blom, 2018; Wang et al., 1995), which relates the ratio of sediment supply to the bifurcates to known model parameters.

We adopt a highly simplified nodal point relation, as the uncertainty related to nodal point relations is large, and available field data to calibrate them are scarce and uncertain. Our nodal point relation relates the ratio of the sediment supply of grain size class k , $S_{k,P}$, of bifurcates W (Waal) and P (Pannerden Canal), to the ratio of their water discharge, Q , multiplied by the prefactor a_k :

$$\frac{S_{k,W}}{S_{k,P}} = a_k \frac{Q_W}{Q_P} \quad (2)$$

where a_k equals 2.73 for both sand fractions, 0.4 for fine gravel, and 0.5 for both coarse gravel fractions. The resulting sediment flux ratios fall within the range of the Frings et al. (2015) estimates of annual sediment flux, and are comparable to the limited amount of field measurements and laboratory experiments (Frings & Kleinhans, 2008).

Sediment management practices are extensive in the lower Rhine River. We include fixed layers (Figure 2a); fine gravel nourishments at rates of 0.1 Mton/a over four 5-km reaches equally distributed between river km 810–855 (Frings et al., 2014) until 2020, beyond which they would cause unwanted aggradation; and dredging over the lowermost 25 km of the river, at an estimated rate of 5,000 m³/a until 2025, when net-removal dredging contracts are set to terminate.

We calibrate the model over the period 2000–2010 against (a) measured channel bed aggradation rates (Figure 2d) and (b) the measured temporal change of flow partitioning at the Pannerden bifurcation (Figure 2e). For the latter, we consider two ranges of water discharge (<1,500 and >2,500 m³/s), corresponding to closure and opening of the weirs downstream of the Pannerden Canal, which is dependent on water discharge at Lobith. Calibration parameters include a spatially variable, piece-wise linear Chézy friction coefficient, the prefactor and critical shear stress in the sediment transport relation, the grain size distribution of the sediment flux at the upstream boundary, and the coefficients a_k of the nodal point relation (Text S4 in Supporting Information S1). The direction of change (aggradation vs. degradation) is generally well captured. The mean absolute difference in aggradation rates is 0.25 cm/a in the German Rhine, and 0.6 cm/a in the Dutch Rhine. The relative error in the ratio of Waal to Bovenrijn discharge is 10%. Sediment fluxes are within the Frings et al. (2019) uncertainty range, albeit on the lower end.

We verify the model against the same variables, over the period 2010–2020 (Figures 2d and 2e). Aggradation rates are only verified for the Dutch Rhine, as bed level data for the German Rhine (river km 640–857) over 2010–2020 is not available to the authors. Verification results are of the same order of accuracy as calibration results.

3. Ongoing Channel Response to Past Human Intervention

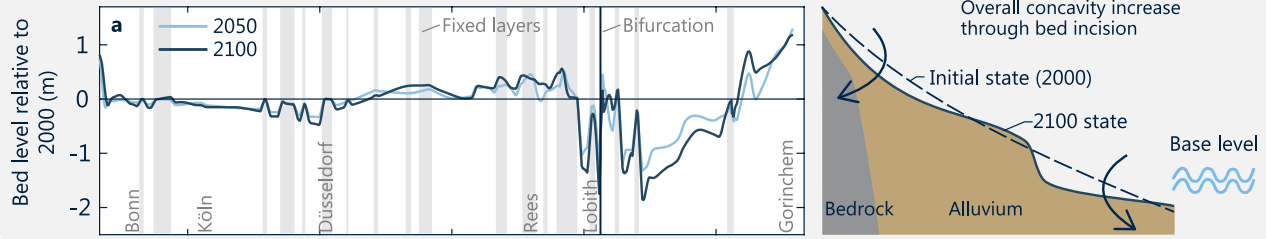
We first address expected bed level change in 2050 and 2100, relative to the initial state (2000) and without climate scenarios (i.e., the reference case, Figure 4a).

Incision rates increase in the downstream direction between river km 640–750, slightly increasing channel slope. Between river km 870–925, incision rates decrease in the downstream direction. The latter slightly decreases channel slope, with a tilting point around river km 925, downstream of which the river aggrades, suggesting an overall increase in concavity, and a continuation of river bed incision trends (Ylla Arbós et al., 2021). This behavior is consistent with historical observations of bed level change, related to an ongoing slope adjustment due to domain-wide channel narrowing in the presence of an upstream bedrock reach (Ylla Arbós et al., 2021). The largest incision rates are observed immediately downstream of fixed layers.

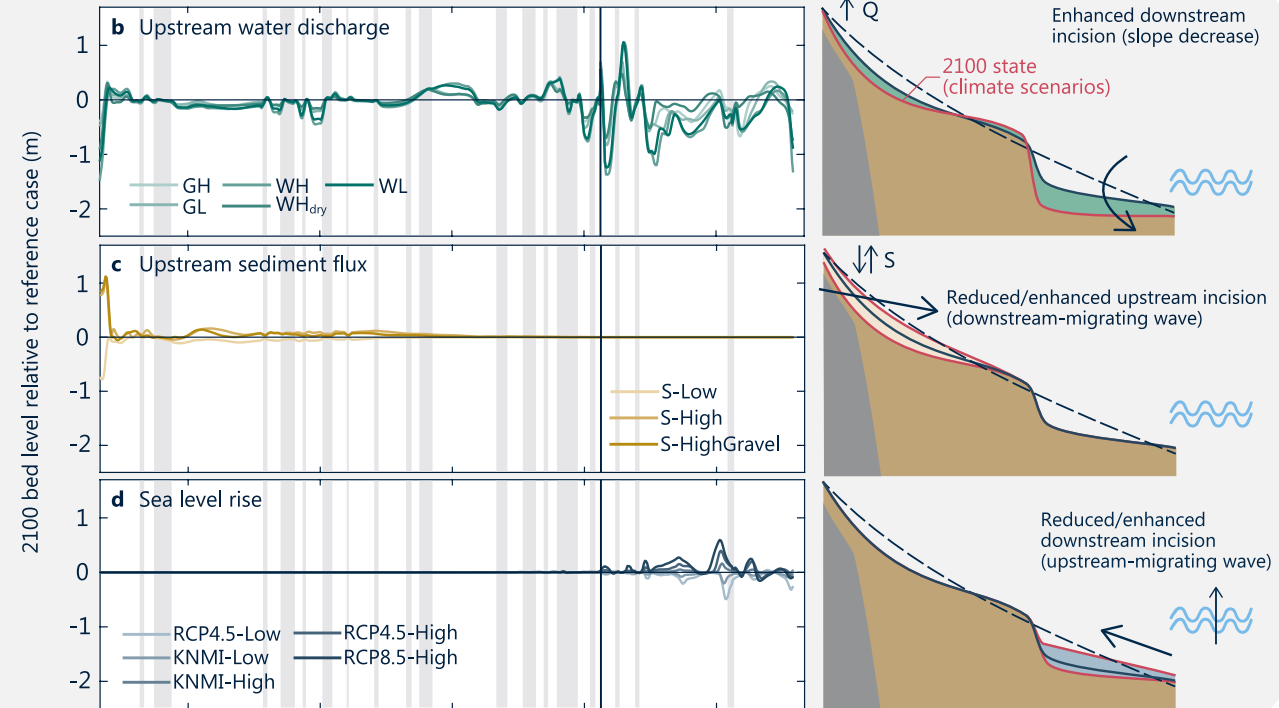
Incision rates range between 0 and 2.5 cm/year up to 2050, and between 0 and 1 cm/year between 2050 and 2100 (Figure 4a). This means that while the channel is expected to continue to incise in the future, incision rates decrease with time as the channel approaches its equilibrium state.

Channel bed incision is less pronounced in the German Rhine (river km 640–857) than in the Dutch Rhine (river km 857–955). The relatively large incision rates in the Dutch Rhine seem to be associated with instability of the Pannerden bifurcation. The steady temporal increase of the fraction of water discharge flowing into the Waal branch (Figure 2e) likely enhances incision downstream from the bifurcation, which further increases the flow rate into the Waal branch. Additionally, the fixed beds have limited river bed incision in the German Rhine and over river km 850–885 (Czapiga et al., 2022; Frings et al., 2014).

Reference case



Climate scenarios (isolated)



Climate scenarios (combined)

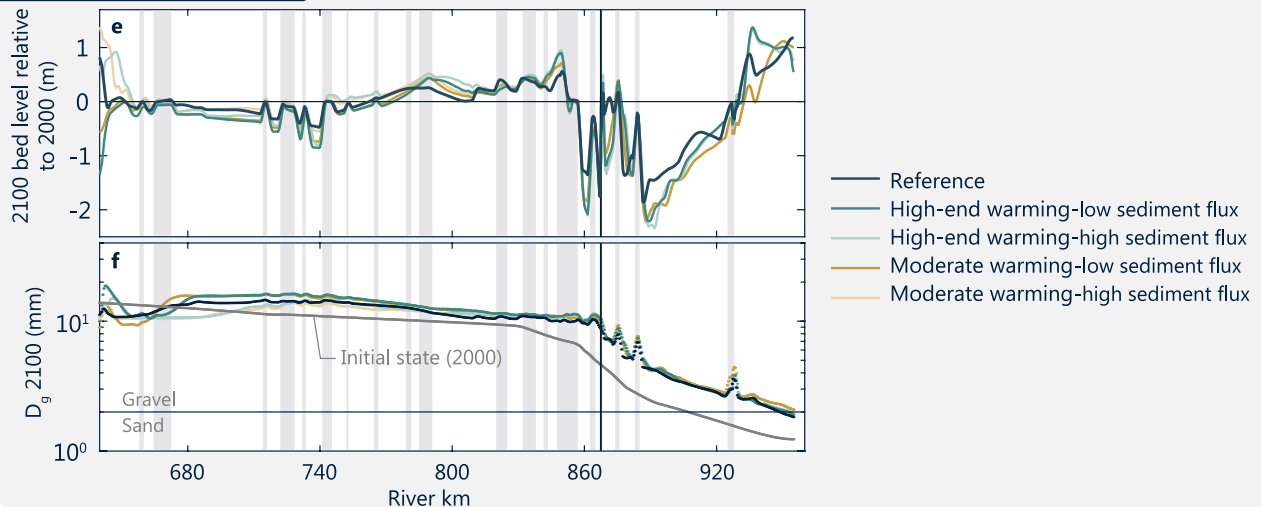


Figure 4. Expected channel response to human intervention and climate change scenarios: (a) bed level relative to 2000 for the reference case. (b–d) Bed level in 2100 relative to the reference case for (isolated) scenarios for the (b) hydrograph, (c) sediment flux, and (d) sea level rise; (e) 2100 bed level relative to 2000 for combined climate scenarios (hydrograph, sediment flux, and sea level rise), and (f) geometric mean bed surface grain size for combined climate scenarios. Schematics to the right-hand side of subplots (a–d) illustrate the response schematically, where arrows indicate main direction of change, and shaded areas in (b–d) indicate the range of change relative to the reference case.

The channel slightly aggrades between river km 770–860. This reach is characterized by a relatively low sediment transport rate in the initial state (Figure S7e in Supporting Information S1). The sediment transport rates upstream of this reach are larger, which creates an aggradational wave migrating in the downstream direction.

The bed surface continues to coarsen (Figure 4f, reference case), which implies that the past coarsening trend continues and the abruptness of the gravel-sand transition has ceased to exist (Frings et al., 2014; Ylla Arbós et al., 2021). Possible explanations of the continued bed surface coarsening include (a) downstream migration of the Rhine gravel-sand transition (Ylla Arbós et al., 2021); (b) temporal reduction of the sediment flux as the channel adjusts to the channelization measures of the past (Figure S7e in Supporting Information S1); (c) continued channel response to past sediment nourishments, carried out primarily before the model initial state in 2000. Channel narrowing has led to a temporary increase of the sediment transport rate. Narrowing does not affect the sediment flux from the upstream part of the basin, but leads to a decreased equilibrium channel slope (and so bed incision) until the sediment transport rate has decreased and equals the upstream sediment flux again.

Despite our simplified treatment of the bifurcation, we observe that (a) sand fractions are preferentially transported into the Waal independently of river discharge, while gravel fractions partition more evenly, and the relative amount of gravel transported into the Panterden Canal increases with discharge; (b) overall, as discharge increases, relatively more sediment is being transported into the Panterden Canal; and (c) the relative amount of sediment transported into the Panterden Canal decreases with time (Text S5 in Supporting Information S1). These observations suggest instability of the Panterden bifurcation.

4. Channel Response to Climate Change: Isolated Climate Scenarios

To assess how climate change adds up to the ongoing response, we adopt scenarios of control change and translate them into model boundary conditions. Here we test different scenarios of a single control at a time. We focus on results for 2100, and mention intermediate changes by 2050. Additional results for 2050 are included in Text S6 in Supporting Information S1. We consider channel response to, subsequently, climate-related hydrograph changes, sediment supply variations, and sea level rise.

Sperna Weiland et al. (2015) use a hydrological model (Hegnauer et al., 2014) to translate precipitation scenarios (KNMI, 2015) into five 50-year synthetic time series of daily river discharge at different stations of the Rhine River, representative of the predicted climate conditions in 2050 and 2085. We consider the discharge station at Köln (river km 687, Figure 1). The Sperna Weiland et al. (2015) scenarios (WH, WH_{dry}, WL, GH, GL, following KNMI, 2015 nomenclature) consist of 15%–50% higher peak flows in winter and 0%–40% lower base flows in summer by 2085. Text S7 in Supporting Information S1 describes how the KNMI (2015) scenarios account for uncertainty in climate predictions.

We use information on the statistics of the flow duration curves (Sperna Weiland et al., 2015) to modify our reference cycled hydrograph. To this end, we estimate the p th-percentile of the discharge for the Sperna Weiland et al. (2015) 2050 and 2085 data, Q_p^{itN} , where the superscript i denotes the scenario, t the time horizon (2050 or 2085), and N is the Sperna Weiland et al. (2015) data. We repeat this for the Sperna Weiland et al. (2015) reference case, Q_p^{refN} . We determine the relative change of the p th-percentile discharge according to Sperna Weiland et al. (2015), F_p^{itN} :

$$F_p^{itN} = \frac{Q_p^{itN}}{Q_p^{refN}} \quad (3)$$

We then multiply each p th-percentile discharge in the hydrograph of our reference case, Q_p^{ref} , by the factor F_p^{itN} to account for climate change effects:

$$Q_p^{it} = F_p^{itN} Q_p^{ref} \quad (4)$$

For intermediate times, we linearly interpolate between values of Q_p^{it} , and linearly extrapolate for values up to 2100.

Our method provides a new hydrograph for each scenario with a new flow duration curve based on climate-related changes in flow statistics. The sequence of flow events is the same as in the reference case. Text S7 in Supporting Information S1 illustrates the method with a workflow chart.

Figure 4b shows how the hydrograph scenarios add to the ongoing channel response in the reference case, in terms of bed level difference in 2100. Water discharge scenarios enhance the ongoing incision by 0–0.35 m (0–0.10 m by 2050) in the German Rhine and 0–1 m (0–0.35 m by 2050) in the Dutch Rhine. This enhanced incision is because all scenarios predict increased moderate to high discharges, which are the most relevant to channel response (Blom et al., 2017), and lead to a smaller equilibrium channel slope. More frequent high flows also increase the relative amount of sediment going into the Pannerden Canal enhancing bifurcation instability (Section 3).

In defining sediment flux scenarios, we assume that the large uncertainty of the Frings et al. (2014) field data (40%–150%, Figure 1) is larger than potential climate-related flux changes. We translate the lower and upper bounds of the uncertainty range into scenarios for the upstream sediment flux. We define three scenarios: low sediment flux (low end of uncertainty range), high sediment flux (high end of uncertainty range), and high gravel flux (high end of uncertainty range for the gravel fractions, and mean values for the sand fractions).

Figure 4c shows the difference in bed level change between the sediment flux scenarios and the reference case, in 2100. The response to changes in the sediment flux starts at the upstream boundary and migrates downstream. By 2100, the adjustment wave has advanced about 200 km (100 km by 2050). Over the upstream end of the domain, higher sediment fluxes reduce river bed incision by 0–0.15 m (0–0.10 m by 2050), and lower fluxes increase it by 0–0.10 m (0–0.05 m by 2050).

We consider five scenarios of sea level rise (Figure 1): the upper and lower end of the KNMI (2015) sea level rise scenarios, the upper and lower end of the RCP 4.5 scenarios, and the upper end of the RCP 8.5 scenarios (IPCC, 2013). Note that future sea level rise largely depends on whether Antarctic ice or Greenland ice melts (Larour et al., 2017). We translate the scenarios into water level at the downstream boundary of our model at Vuren with Equation 1, adjusting d_s based on the scenarios.

Figure 4d shows that for rates of sea level rise larger or smaller than that of the reference case, the 2100 response consists, respectively, of reduced incision by 0–0.30 m (0–0.05 m by 2050), or enhanced incision by 0–0.25 m (0–0.10 m by 2050). Sea level rise leads to an upstream-migrating wave, covering about 90 km by 2100 (50 km by 2050), up to the Pannerden bifurcation (river km 867.5).

The limited influence of sea level rise on channel response can be explained by the fact that the rate of sea level rise is an order of magnitude smaller than that of the bed level change in the reference case. Bifurcation partitioning trends remain unaffected by sea level rise in 2100. Nonetheless, as sea level has risen since before 2000 (IPCC, 2022), the initial state of the river system is already affected by past sea level rise.

5. Channel Response to Climate Change: Combined Climate Scenarios

To assess the effects of combined scenarios, we perform model runs for several scenario combinations, associated with the smallest and largest predicted temperature and precipitation increase by 2100 (IPCC, 2013). This results in two hydrograph-sea-level-rise scenario combinations, hereafter referred to as moderate and high-end warming scenarios (respectively, scenarios GL-RCP4.5-Low and WH-RCP8.5-High). As sediment flux scenarios are assumed to be independent of climate scenarios, we test the climate scenario combinations for both the lower and upper bound of the sediment flux scenarios (S-Low and S-High), resulting in four scenario combinations.

Figure 4e shows the bed level difference between 2100 and the initial state (2000) for the reference case and the combined scenarios. Overall, the ongoing response to past channelization measures is dominant, and climate scenarios further enhance incision by 0.15–0.70 m (0–0.30 m by 2050). Furthermore, these results suggest an overall dominance of water discharge scenarios over sea level rise in channel response to climate change. The bed surface coarsening and the downstream-migrating coarsening wave are not significantly affected by climate scenarios (Figure 4f).

Our results agree with field observations and modeling efforts regarding climate change effects in engineered rivers (e.g., Muñoz et al., 2018; Verhaar et al., 2010), and confirm the key role of engineering measures in channel response, even in the presence of notable climate forcing. The relative importance of extreme flow events may, however, be significant in bifurcating river systems. In particular, peak flows may lead to substantial sediment deposition in one bifurcate, which may alter flow and sediment partitioning at the bifurcation, affecting future channel response (Chowdhury et al., 2023a).

6. Conclusions

We have developed a strategy to assess climate-related impact on river channels. Our model aims to identify large-scale and multi-decadal trends of channel response, and therefore only provides order-of-magnitude expected change. Our conceptual analysis of channel response to isolated and combined climate scenarios provides clues to how engineered rivers worldwide respond to climate change.

Our results suggest that (past) human intervention is the main driver of channel response in the lower Rhine River over the 21st century, leading to channel bed incision.

Climate forcing enhances this incision, mostly due to increased moderate discharges, which decreases the equilibrium channel slope. Sea level rise mildly reduces river bed incision in the downstream part of the domain.

While channel response to human intervention slows down as the river approaches its equilibrium state, channel response to climate change accelerates, as changes in controls accelerate. The relative importance of climate forcing on channel response therefore increases with time. Bifurcation dynamics are expected to play a key role in future channel adjustment.

The uncertainty related to climate projections and measured data being high, our highly schematized one-dimensional model proves to be a useful, and computationally cheap tool to assess channel response at large spatio-temporal scales, for a wide range of scenarios.

Data Availability Statement

The input of our model is based on field data. Bed level data is accessible at Quick et al. (2019) for the German Rhine, and at Ylla Arbós (2021) for the Dutch Rhine. Main channel width data is obtained from Google Earth (<https://earth.google.com/web/>). Floodplain width data is available from BfG (2020b). Grain size data is available at the SedDB database for the German Rhine (BfG, 2020a), and in Ylla Arbós (2023) for the Dutch Rhine. Historical discharge data is available via BfG (2020b) and Chowdhury et al. (2023b). Water level data is available at <https://waterinfo.rws.nl>. Model input files and results are available at Ylla Arbós (2023).

References

- Arkesteijn, L., Blom, A., Czupiga, M. J., Chavarrías, V., & Labeur, R. J. (2019). The quasi-equilibrium longitudinal profile in backwater reaches of the engineered alluvial river: A space-marching method. *Journal of Geophysical Research: Earth Surface*, *124*(11), 2542–2560. <https://doi.org/10.1029/2019JF005195>
- Arkesteijn, L., Blom, A., & Labeur, R. J. (2021). A rapid method for modeling transient river response under stochastic controls with application to sea level rise and sediment nourishment. *Journal of Geophysical Research: Earth Surface*, *126*(12), e2021JF006177. <https://doi.org/10.1029/2021JF006177>
- BfG. (2020a). BfG sediment datenbank. Retrieved from <https://geoportal.bafg.de/sedddb>
- BfG. (2020b). The Global Runoff Data Centre. Retrieved from <https://www.bafg.de/GRDC>
- Blom, A., Arkesteijn, L., Chavarrías, V., & Viparelli, E. (2017). The equilibrium alluvial river under variable flow and its channel-forming discharge. *Journal of Geophysical Research: Earth Surface*, *122*(10), 1924–1948. <https://doi.org/10.1002/2017JF004213>
- Blom, A., Viparelli, E., & Chavarrías, V. (2016). The graded alluvial river: Profile concavity and downstream fining. *Geophysical Research Letters*, *43*(12), 6285–6293. <https://doi.org/10.1002/2016GL068898>
- Blöschl, G., Hall, J., Viglione, A., Perdigão, R. A., Parajka, J., Merz, B., et al. (2019). Changing climate both increases and decreases European river floods. *Nature*, *573*(7772), 108–111. <https://doi.org/10.1038/s41586-019-1495-6>
- Bolla Pittaluga, M., Repetto, R., & Tubino, M. (2003). Channel bifurcation in braided rivers: Equilibrium configurations and stability. *Water Resources Research*, *39*(3), 1046. <https://doi.org/10.1029/2001WR001112>
- Bresse, J. A. C. (1860). *Cours de mécanique appliquée, professé à l'École des ponts et chaussées* (Vol. 2). Mallet-Bachelier. (In French).
- Chen, X., Zhang, X., Church, J. A., Watson, C. S., King, M. A., Monselesan, D., et al. (2017). The increasing rate of global mean sea-level rise during 1993–2014. *Nature Climate Change*, *7*(7), 492–495. <https://doi.org/10.1038/nclimate3325>
- Chowdhury, M. K., Blom, A., Ylla Arbós, C., Verbeek, M. C., Schropp, M. H. I., & Schielen, R. M. J. (2023a). Semicentennial response of a bifurcation region in an engineered river to peak flows and human interventions. *Water Resources Research*, *59*, e2022WR032741. <https://doi.org/10.1029/2022WR032741>
- Chowdhury, M. K., Blom, A., Ylla Arbós, C., Verbeek, M. C., Schropp, M. H. I., & Schielen, R. M. J. (2023b). *Bed elevation, bed surface grain size (D50 and D90), and water discharge- Waal, Pannerden Channel, Nederrijn, and IJssel, 1928-2020* (Version 4) [Dataset]. 4TU.ResearchData. <https://doi.org/10.4121/19650873.v4>
- Czapiga, M. J., Blom, A., Viparelli, E., & Asce, M. (2022). Sediment nourishments to mitigate channel bed incision in engineered rivers. *Journal of Hydraulic Engineering*, *148*(6), 04022009. [https://doi.org/10.1061/\(ASCE\)HY.1943-7900.0001977](https://doi.org/10.1061/(ASCE)HY.1943-7900.0001977)
- De Saint-Venant, A. B. (1871). Théorie et équations générales du mouvement non permanent des eaux courantes. *Comptes Rendus des séances de l'Académie des Sciences, Paris, France, Séance, 17*(73), 147–154. (In French).
- De Vriend, H. (2015). The long-term response of rivers to engineering works and climate change. *Proceedings of the Institution of Civil Engineers - Civil Engineering*, *168*(3), 139–144. <https://doi.org/10.1680/cien.14.00068>

Acknowledgments

This study is part of the research program Rivers2Morrow, financed by the Dutch Ministry of Infrastructure and Water Management. We thank Regina Patzwahl and Victor Chavarrías for their help in understanding and modeling the system. We thank reviewers Andy Wickert and Chenge An for their valuable input in improving this manuscript.

- De Vries, M. (1994). Unsolved problems in one-dimensional morphological models. In *IAHR-AD. IAHR. Deltates*. (2012a). Morphology and sediment transport – Technical reference manual SOBEK RE 2.52.008. Deltates. (2012b). Technical reference manual SOBEK RE 2.52.008- FLOW.
- Emerson, J. W. (1971). Channelization: A case study. *Science*, *173*(3994), 325–326. <https://doi.org/10.1126/science.173.3994.325>
- Exner, F. M. (1925). Über die wechselwirkung zwischen wasser und geschlebe in flüssen. *Akademie der Wissenschaften in Wien Mathematische Naturwissenschaftliche Klasse*, *134*(2a), 165–204. (In German).
- Exner, F. M. (1931). Zur dynamik der bewegungsformen auf der erdoberfläche. *Ergebnisse der kosmischen Physik*, *1*, 373–445. (In German).
- Frings, R. M., Banhold, K., & Evers, I. (2015). *Sedimentbilanz des Oberen Rheindeltas für den Zeitraum 1991–2010*. Aachen.
- Frings, R. M., Döring, R., Beckhausen, C., Schüttrumpf, H., & Vollmer, S. (2014). Fluvial sediment budget of a modern, restrained river: The lower reach of the Rhine in Germany. *CATENA*, *122*, 91–102. <https://doi.org/10.1016/j.catena.2014.06.007>
- Frings, R. M., Hillebrand, G., Gehres, N., Banhold, K., Schriever, S., & Hoffmann, T. (2019). From source to mouth: Basin-scale morphodynamics of the Rhine River. *Earth-Science Reviews*, *196*, 102830. <https://doi.org/10.1016/j.earscirev.2019.04.002>
- Frings, R. M., & Kleinhans, M. G. (2008). Complex variations in sediment transport at three large river bifurcations during discharge waves in the river Rhine. *Sedimentology*, *55*(5), 1145–1171. <https://doi.org/10.1111/j.1365-3091.2007.00940.x>
- Gao, W., Li, D., Wang, Z. B., Nardin, W., Shao, D., Sun, T., et al. (2020). The longitudinal profile of a prograding river and its response to sea level rise. *Geophysical Research Letters*, *47*(21), e2020GL090450. <https://doi.org/10.1029/2020GL090450>
- Harmar, O. P., Clifford, N. J., Thorne, C. R., & Biedenbarn, D. S. (2005). Morphological changes of the Lower Mississippi River: Geomorphological response to engineering intervention. *River Research and Applications*, *21*(10), 1107–1131. <https://doi.org/10.1002/rra.887>
- Hegnauer, M., Beersma, J., Van den Boogaard, H., Buishand, T., & Passchier, R. (2014). *Generator of rainfall and discharge extremes (GRADE) for the Rhine and Meuse basins*. Final report of GRADE 2.0. Deltates.
- Hirano, M. (1971). River-bed degradation with armoring. *Proceedings of the Japan Society of Civil Engineers*, *1971*(195), 55–65. https://doi.org/10.2208/jscej1969.1971.195_55
- IPCC. (2013). *Climate change 2013: The physical science basis. Contribution of Working Group I to the fifth assessment report of the Intergovernmental Panel on Climate Change*. Cambridge University Press.
- IPCC. (2022). *Sea level rise and implications for low-lying islands, coasts and communities*. Cambridge University Press. <https://doi.org/10.1017/9781009157964.006>
- KNMI. (2015). *KNMI '14 climate scenarios for The Netherlands*. Royal Netherlands Meteorological Institute. Retrieved from <http://www.climate-scenarios.nl/>
- Larour, E., Ivins, E. R., & Adhikari, S. (2017). Should coastal planners have concern over where land ice is melting? *Science Advances*, *3*(11), e1700537. <https://doi.org/10.1126/SCIADV.1700537>
- Liu, C., Sui, J., He, Y., & Hirshfield, F. (2013). Changes in runoff and sediment load from major Chinese rivers to the Pacific Ocean over the period 1955–2010. *International Journal of Sediment Research*, *28*(4), 486–495. [https://doi.org/10.1016/S1001-6279\(14\)60007-X](https://doi.org/10.1016/S1001-6279(14)60007-X)
- Mackin, J. H. (1948). Concept of the graded river. *GSA Bulletin*, *59*(5), 463–512. [https://doi.org/10.1130/0016-7606\(1948\)59\[463:cotgr\]2.0.co;2](https://doi.org/10.1130/0016-7606(1948)59[463:cotgr]2.0.co;2)
- Milliman, J. D., Farnsworth, K. L., Jones, P. D., Xu, K. H., & Smith, L. C. (2008). Climatic and anthropogenic factors affecting river discharge to the global ocean, 1951–2000. *Global and Planetary Change*, *62*(3–4), 187–194. <https://doi.org/10.1016/j.gloplacha.2008.03.001>
- Muñoz, S. E., Giosan, L., Therrell, M. D., Remo, J. W., Shen, Z., Sullivan, R. M., et al. (2018). Climatic control of Mississippi River flood hazard amplified by river engineering. *Nature*, *556*(7699), 95–98. <https://doi.org/10.1038/nature26145>
- Paola, C., & Leeder, M. (2011). In modelling, simplicity isn't simple. *Nature*, *469*(7328), 38–39. <https://doi.org/10.1038/469038a>
- Parker, G., & Klingeman, P. C. (1982). On why gravel bed streams are paved. *Water Resources Research*, *18*(5), 1409–1423. <https://doi.org/10.1029/WR018I005P01409>
- Parker, G., Klingeman, P. C., & McLean, D. G. (1982). Bedload and size distribution in paved gravel-bed streams. *Journal of the Hydraulics Division*, *108*(4), 544–571. <https://doi.org/10.1061/JYCEAJ.0005854>
- Quick, I., König, F., Baulig, Y., Schriever, S., & Vollmer, S. (2019). Evaluation of depth erosion as a major issue along regulated rivers using the classification tool Valmorph for the case study of the Lower Rhine. *International Journal of River Basin Management*, *18*(2), 1–16. <https://doi.org/10.1080/15715124.2019.1672699>
- Schielen, R. M. J., & Blom, A. (2018). A reduced complexity model of a gravel-sand river bifurcation: Equilibrium states and their stability. *Advances in Water Resources*, *121*, 9–21. <https://doi.org/10.1016/j.advwatres.2018.07.010>
- Sloff, K., & Mosselman, E. (2012). Bifurcation modelling in a meandering gravel–sand bed river. *Earth Surface Processes and Landforms*, *37*(14), 1556–1566. <https://doi.org/10.1002/ESP.3305>
- Sperna Weiland, F., Hegnauer, M., Bouaziz, L., & Beersma, J. (2015). *Implications of the KNMI'14 climate scenarios for the discharge of the Rhine and Meuse*. Deltates.
- Surian, N., & Rinaldi, M. (2003). Morphological response to river engineering and management in alluvial channels in Italy. *Geomorphology*, *50*(4), 307–326. [https://doi.org/10.1016/S0169-555X\(02\)00219-2](https://doi.org/10.1016/S0169-555X(02)00219-2)
- Van Vuren, S., Paarlberg, A., & Havinga, H. (2015). The aftermath of “Room for the River” and restoration works: Coping with excessive maintenance dredging. *Journal of Hydro-environment Research*, *9*(2), 172–186. <https://doi.org/10.1016/J.JHER.2015.02.001>
- Verhaar, P. M., Biron, P. M., Ferguson, R. I., & Hoey, T. B. (2010). Numerical modelling of climate change impacts on Saint-Lawrence River tributaries. *Earth Surface Processes and Landforms*, *35*(10), 1184–1198. <https://doi.org/10.1002/esp.1953>
- Verhaar, P. M., Biron, P. M., Ferguson, R. I., & Hoey, T. B. (2011). Implications of climate change in the twenty-first century for simulated magnitude and frequency of bed-material transport in tributaries of the Saint-Lawrence River. *Hydrological Processes*, *25*(10), 1558–1573. <https://doi.org/10.1002/hyp.7918>
- Wang, Z. B., De Vries, M., Fokink, R. J., & Langerak, A. (1995). Stability of river bifurcations in 1D morphodynamic models. *Journal of Hydraulic Research*, *33*(6), 739–750. <https://doi.org/10.1080/00221689509498549>
- Ylla Arbós, C. (2021). Bed elevation and bed surface grain size (D50) Bovenrijn and Waal, 1926–2020 (Version 2) [Dataset]. 4TU.ResearchData. <https://doi.org/10.4121/13065359.V2>
- Ylla Arbós, C. (2023). Schematized model of the lower Rhine River (2000–2100) - input and results (Version 1) [Dataset]. 4TU.ResearchData. <https://doi.org/10.4121/21763112.V1>
- Ylla Arbós, C., Blom, A., Viparelli, E., Reneerkens, M., Frings, R. M., & Schielen, R. M. J. (2021). River response to anthropogenic modification: Channel steepening and gravel front fading in an incising river. *Geophysical Research Letters*, *48*(4), e2020GL091338. <https://doi.org/10.1029/2020GL091338>
- Zaprowski, B. J., Pazzaglia, F. J., & Evenson, E. B. (2005). Climatic influences on profile concavity and river incision. *Journal of Geophysical Research*, *110*(F3), 3004. <https://doi.org/10.1029/2004JF000138>

References From the Supporting Information

- Becker, A. (2017). *1D2D model of the Lower Rhine and the Upper Dutch Rhine branches between Andernach and Nijmegen, Arnhem and Zutphen*. (Tech. Rep.). Deltares.
- BfG. (2020). IKSR Rheinatlant. Retrieved from <https://geoportal.bafg.de/arcportal/apps/webappviewer/index.html?id=b6085b53b6d84cd39cff4b5eb7f3f40>
- Carling, P. A., Gözl, E., Orr, H. G., & Radecki-Pawlik, A. (2000). The morphodynamics of fluvial sand dunes in the River Rhine, near Mainz, Germany. I. Sedimentology and morphology. *Sedimentology*, 47(1), 227–252. <https://doi.org/10.1046/j.1365-3091.2000.00290.x>
- D'Errico, J. (2009). *SLM-shape language modeling*. Mathworks. Retrieved from <http://www.mathworks.com/matlabcentral/fileexchange/24443-slm-shape-language-modeling>
- Egiazaroff, I. V. (1965). Calculation of nonuniform sediment concentrations. *Journal of the Hydraulics Division*, 91(4), 225–247. <https://doi.org/10.1061/JYCEAJ.0001277>
- Engelund, F. (1966). Hydraulic resistance of alluvial streams. *Journal of the Hydraulics Division*, 92(2), 315–326. <https://doi.org/10.1061/JYCEAJ.0001417>
- Engelund, F. (1977). Hydraulic resistance for flow over dunes. *Progress Reports*, 44, 19M20.
- Haque, M. I., & Mahmood, K. (1983). Analytical determination of form friction factor. *Journal of Hydraulic Engineering*, 109(4), 590–610. [https://doi.org/10.1061/\(ASCE\)0733-9429\(1983\)109:4\(590\)](https://doi.org/10.1061/(ASCE)0733-9429(1983)109:4(590))
- Hazeleger, W., Wang, X., Severijns, C., Ștefănescu, S., Bintanja, R., Sterl, A., et al. (2012). EC-Earth V2.2: Description and validation of a new seamless Earth system prediction model. *Climate Dynamics*, 39(11), 2611–2629. <https://doi.org/10.1007/S00382-011-1228-5/FIGURES/17>
- IIASA. (2009). RCP database. Retrieved from <https://tntcat.iiasa.ac.at/RcpDb/>
- Julien, P., Asce, M., Klaassen, G., Ten Brinke, W., & Wilbers, A. (2002). Case study: Bed resistance of Rhine River during 1998 flood. *Journal of Hydraulic Engineering*, 128(12), 1042–1050. [https://doi.org/10.1061/\(ASCE\)0733-9429\(2002\)128:12\(1042\)](https://doi.org/10.1061/(ASCE)0733-9429(2002)128:12(1042))
- Karim, F. (1999). Bed-form geometry in sand-bed flows. *Journal of Hydraulic Engineering*, 125(12), 1253–1261. [https://doi.org/10.1061/\(ASCE\)0733-9429\(1999\)125:12\(1253\)](https://doi.org/10.1061/(ASCE)0733-9429(1999)125:12(1253))
- Lenderink, G., Van den Hurk, B., Tank, A. K., Van Oldenborgh, G., Van Meijgaard, E., De Vries, H., & Beersma, J. (2014). Preparing local climate change scenarios for The Netherlands using resampling of climate model output. *Environmental Research Letters*, 9(11), 115008. <https://doi.org/10.1088/1748-9326/9/11/115008>
- Lindström, G., Johansson, B., Persson, M., Gardelin, M., & Bergström, S. (1997). Development and test of the distributed HBV-96 hydrological model. *Journal of Hydrology*, 201(1–4), 272–288. [https://doi.org/10.1016/S0022-1694\(97\)00041-3](https://doi.org/10.1016/S0022-1694(97)00041-3)
- Lokin, L. R., Warmink, J. J., Bomers, A., & Hulscher, S. J. M. H. (2022). River dune dynamics during low flows. *Geophysical Research Letters*, 49(8), e2021GL097127. <https://doi.org/10.1029/2021GL097127>
- Meyer-Peter, E., & Müller, R. (1948). Formulas for bed-load transport. In *IAHR 2nd meeting, Stockholm, Appendix 2*.
- Rijkswaterstaat. (n.d.). Waterinfo. Retrieved from <https://waterinfo.rws.nl>
- RiverLab. (2020). 1D model of the Dutch Rhine River branches (Rijntakken). Retrieved from <https://oss.deltares.nl/web/riverlab-models/-/schematization-of-the-bifurcation-at-pannerden-available>
- Van Rijn, L. C. (1993). *Principles of sediment transport in rivers, estuaries and coastal seas* (Vol. 1006). Aqua Publications Amsterdam.
- Vanouï, V. A., & Hwang, L.-S. (1967). Relation between bed forms and friction in streams. *Journal of the Hydraulics Division*, 93(3), 121–144. <https://doi.org/10.1061/JYCEAJ.0001607>
- Warmink, J. J., Booij, M. J., Van der Klis, H., & Hulscher, S. J. M. H. (2013). Quantification of uncertainty in design water levels due to uncertain bed form roughness in the Dutch river Waal. *Hydrological Processes*, 27(11), 1646–1663. <https://doi.org/10.1002/HYP.9319>
- Wessem, J. M. V., & Laffin, M. K. (2020). Regional atmospheric climate model 2 (RACMO2), version 2.3p2. *Zenodo*. <https://doi.org/10.5281/zenodo.3677642>
- Wilbers, A. W., & Ten Brinke, W. B. (2003). The response of subaqueous dunes to floods in sand and gravel bed reaches of the Dutch Rhine. *Sedimentology*, 50(6), 1013–1034. <https://doi.org/10.1046/j.1365-3091.2003.00585.x>
- Yalin, M. S. (1964). Geometrical properties of sand wave. *Journal of the Hydraulics Division*, 90(5), 105–119. <https://doi.org/10.1061/JYCEAJ.0001097>